NOTICE

CERTAIN DATA CONTAINED IN THIS DOCUMENT MAY BE DIFFICULT TO READ IN MICROFICHE PRODUCTS.

CONF-910

SAND--90-2334C

DE91 005309

DEC 3 3 1990

DISCLAIMER

ABSTRACT

This paper describes preliminary interpretation of in-situ pressure and flow measurements of the Salado Formation at the Waste Isolation Pilot Plant (WIPP). The WIPP facility is located 660 m underground in the Salado, a bedded salt deposit. Shut-in pressure tests were conducted prior to, and subsequent to, the mining of a circular drift in order to evaluate excavation effects on pore pressure, permeability, and host rock heterogeneity. Borehole deformation was measured during these tests and used to correct for changes in the test region volume due to salt creep effects.

Preliminary pre-excavation results indicate that the flow properties of this layered host rock are heterogeneous. Resulting pore pressures range from 1 to 14 MPa and permeabilities range from below measurable to about 1 nanodarcy. Normalized borehole diameter change rates were between -4 and 63 microstrains/day.

Shut-in pressures and borehole diameters in all test boreholes were affected by the excavation of Room Q coincident with the advances of the boring machine. Preliminary results from post-excavation test results show decreased pore pressures compared to pre-excavation values.

INTRODUCTION

The Waste Isolation Pilot Plant, located near Carlsbad, New Mexico, is the U. S. Department of Energy planned repository for transuranic waste generated by defense programs. The Salado Formation bedded salt deposit was chosen for the repository because of salt's natural ability to flow, or creep, over time under the effects of stress or heat: rooms would be mined in the salt, waste would be stored in the rooms and, over time, the salt would deform to seal the rooms thus encapsulating and isolating the waste. As part of Sandia National Laboratories' efforts to provide detailed geotechnical understanding of the WIPP site and assess the suitability of salt for long-term waste isolation, tests are being conducted 660 m underground in the Salado Formation. Pore pressure, brine flow and borehole deformation (closure) rate test results are designed to support mechanistic model development and evaluation.

The polycrystalline Salado salt contains small quantities of brine, on the order of 0.1 to 1% total volume, in intragranular fluid inclusions and as intergranular (pore) fluid. It is important to quantify the amount of brine in the formation and to determine the mobility and rate of movement of the brine because the accumulation of significant quantities of brine in the repository might lead to a number of potential problems that could affect the salt's ability to isolate waste. These potential problems include retardation of salt creep effects, gas generated by anoxic corrosion of metal waste canisters, and radionuclide transport by brine.

The tests discussed in this report were designed to provide information on host rock mechanical properties and fluid flow properties and are part of a large-scale integrated brine inflow experiment. Specifically, tests were run to determine pore pressure and permeability and collect information about the relative heterogeneity of the salt. Pore pressure data is important in determining the interconnectedness of fluid-filled pores to determine the fluid flow mechanism(s) and evaluate the amount of brine that could potentially flow into excavations. Likewise, permeability information can be used to determine the appropriate mechanistic model for brine flow within the Salado and from the salt to excavations. Permeability values from other in-situ tests in the Salado, estimated using a poroelastic model, range from 1 to 10 nanodarcies.

References and illustrations at end of paper.

MASTER

Fifteen boreholes were drilled and instrumented at the entrance to Room Q, a 110 m long by 3 m diameter circular drift. Three arrays of 5 boreholes are located vertically above, vertically below, and horizontally outward from Room Q (see Figures 1 and 2). Pressure, brine inflow, and closure rate data are monitored in the uncased test zones at the end of each borehole. These brine-filled test regions are isolated from the rest of the borehole using inflatable packer systems. Two-axis borehole deformation gages are installed in each of the test regions to distinguish between the effects of borehole closure and those of brine flow. Temperatures are monitored on the borehole walls and on the tool mandrels outside the test region.

Instrumentation was installed, and monitoring was initiated prior to the excavation of Room Q to determine the undisturbed in-situ conditions, the effects of the excavation process, and the resulting conditions that occurred subsequent to excavation. Data from these tests are used to estimate the formation pore pressure, permeability, and degree of heterogeneity.

The experiment design and measurement system will be described followed by a presentation of the test procedure and analytical method. Then, pre-excavation, excavation, and post-excavation results will be discussed and conclusions listed.

TEST METHOD

The test region locations of the 15 pressure/flow/closure measurement systems are shown in Figure 1. Each test region is located at an axial distance of 22.9 m measured from the entrance to Room Q. The radial locations of the test regions relative to the centerline axis of Room Q are shown in Figure 2; five test positions are located vertically above, five are located vertically below, and five are located horizontally outward from the room. The three outer-most boreholes, QPP01, QPP11, and QPP21, are 10.2 cm in diameter and uncased. The remaining 12 boreholes have a 3.8 cm diameter test region that is stepped down from a cased 10.2 cm borehole.

Figure 2 also identifies the stratigraphic layer and corresponding lithology intersected by each borehole test region. In the vicinity of Room Q, the Salado Formation is predominately halite. However, layers of anhydrite, polyhalite, clays, and argillaceous halite are found sandwiched between halite units. The 15 boreholes were not cored, so hole surveys were used to estimate the stratigraphic layer intersected by each borehole.

All fifteen boreholes were air-drilled from the instrument area shown on Figure 1 in early 1989. The holes were drilled, cased, and grouted with cement between February 22, 1989 and March 23, 1989 and the tools were installed between April 5, 1989 and the beginning of May 1989. Data monitoring began on April 25, 1989 and Room Q was excavated between July 12, 1989 and August 8, 1989.

MEASUREMENT SYSTEMS

A schematic diagram of the test measurement system is presented in Figure 3. The system consists of four major parts: a) the single- or dual-packer and closure gage assembly, b) the flow control and data acquisition system, c) the pressurized nitrogen and inflatable packer water supply cylinders, and d) the data acquisition computer and printer.

The dual-packer and closure gage assembly, shown in Figure 3a, is installed at the uncased end of a test borehole. Both a test region and a guard region are isolated using the dual-packer system. In some boreholes, a single-packer system is used and there is no guard zone. Table 1 summarizes the pressure/flow/closure test system configurations for each borehole.

The two-axis borehole deformation gage is located within the test region and measures changes in borehole diameter with an accuracy of 0.0002 cm. The test and guard regions and the packers are connected to the flow-control and data acquisition system using type 316 seamless stainless steel tubing.

The flow control and data acquisition system cabinet is illustrated in Figure 3b. This part of the measurement system controls the pressures within, and flow rates to, the test and guard regions, the brine accumulators, and the packers. The pressure transducers and brine accumulators are housed inside the cabinet. Test and guard region pressures are measured to within 0.001 MPa and brine accumulation is measured to within 0.1 cc. These transducers are calibrated to a National Institute for Standards and Technology reference. Individual packer pressures are monitored for operational purposes only and are not calibrated to these standards. The maximum working pressure is 15 MPa.

Test and guard region pressures are adjusted using a brine supply system pressurized by the nitrogen cylinders as shown in Figure 3c. Pressures in the fresh-water filled inflatable packers are adjusted by varying the pressure on the nitrogen supply for the packer-water cylinders.

A Leading Edge Model D computer is used to record all pressure, brine accumulation, and closure data on a hard disk. This part of the measurement system is housed in the Computer/Printer Cabinet as shown schematically in Figure 3d. A total of 90 parameters are measured at the 15 boreholes and any can be selectively displayed on the monitor to aid in test set-up or data interpretation. These data are printed out and/or copied to a floppy disk for permanent storage.

TEST PROCEDURES

Two types of tests are performed: shut-in pressure tests and constant-pressure flow tests. The shut-in pressure test data are used to estimate formation pore pressure and permeability and the data from the constant-pressure flow tests are used to infer permeability.

Shut-in Pressure Tests

A shut-in test is initiated by setting the pressure in the test and/or guard region to a specified value. A valve on the line from the pressure source to the region is then closed and the pressure response with time is monitored.

Pore pressure values can be estimated from the shut-in pressure test data provided that the test duration is of sufficient length to allow the final borehole pressure to approach the far-field pore pressure. Permeability values can also be determined from these data provided that the transient response takes place over a time period that significantly exceeds the time required for a pressure disturbance to propagate beyond any damage zone surrounding the borehole. This latter requirement can only be satisfied if the shut-in test has been preceded by a production period whose duration depends on parameters such as the formation diffusivity, test region storage capacity, and borehole diameter. Test durations are necessarily long for this low permeability salt formation and lengthy production periods are required.

Constant-Pressure Flow Tests

During a constant-pressure flow test, the pressure in the test region or guard region is maintained at a specified value and the fluid flow volume into or out of the region is measured as a function of time. Permeability values can then be inferred from these data. This is the preferred method for measuring permeability because the tests can be run for a long enough period to ensure that the associated pressure disturbance has penetrated beyond any possible damage zone. In addition, since these tests are run under constant pressure conditions, tool compliance effects are not a factor.

Unfortunately, there are limited constant-pressure flow data so far from our tests. With the exception of data taken from borehole QPP23 during the excavation, none will be reported in this paper. Due to the long time periods required to perform constant-pressure flow tests, all the time available between the initiation of these borehole tests and the excavation of Room Q was used for performing the test region shut-in tests. A few flow tests were attempted in guard regions, but the flow measurement system did not operate properly. The flow measurement system has since been replaced for use in future tests.

Borehole Deformation

The borehole diameter deformation is measured over time so that measured flow rates or flow rates implied by the shut-in pressure test data can be corrected for changes in the test region volume. The deformation measurements are made in the test region of each borehole using a system composed of two orthogonal diameter gages. It is recognized that the test region's length may increase as a result of the packer element sliding with respect to the mounting mandrel. To date, this effect has not been measured, but future tests systems planned for Room Q will incorporate an axial borehole gage.

ANALYSIS

Formation Pore Pressure

Formation pore pressures were calculated from shut-in pressure test data. Three types of pressure responses were observed: 1) a classic pressure build-up and stabilization, 2) a constant pressure equal to that initially set in the test region, and 3) a rapid equilibration to a test-region-specific anomalously low pressure independent of the initial pressure set in the test region.

For shut-in tests in which the pressure versus time history followed the classic build-up profile, the formation pore pressure was estimated using a Horner-like plot [1,2]. For example, Figure 4 shows the raw shut-in pressure data from QPP03 and Figure 5 shows the corresponding Horner-like plot. In Figure 5, the time ($time_p$) was taken equal to the time the borehole was open prior to the initiation of the shut-in test. The formation pore pressure corresponds to the extrapolated value of pressure at ($time_p$ + time)/time = 1.0.

An example of a shut-in test data response where the pressure remained constant following the initial changes resulting from system compliance is shown in Figure 6 for QPP15. No reasonable estimate of pore pressure can be determined from these data since the formation permeability is so low that meaningful pressure changes did not occur even in the 30 day test performed at a pressure of 6.5 MPa.

Figure 7 shows shut-in data from QPP02. In this case the test region pressure equilibrated at about 1.0 MPa, independent of the initial pressure set in the test region.

In some cases the permeability was so low that excavation of Room Q occurred before sufficient data were obtained. In other cases, such as for QPP23, boreholes were incapable of maintaining high pressure thereby producing results similar to those shown on Figure 8. For these cases, the lower pore pressure values reported in Table 2 correspond to the maximum measured pressures and the upper values were determined from extrapolations of the Horner-like plots.

Because borehole deformation can significantly influence pressure responses, it must be considered when interpreting shut-in or flow data. Decreasing borehole diameter can produce test results that are indistinguishable from those obtained from brine flow into the borehole. The effect of an increasing borehole diameter is exactly opposite. For example, if a borehole is closing and the formation is permeable, the final equilibrium pressure is a measure of the mechanical characteristics of the formation and not a measure of the pore pressure. If the borehole is opening, the formation pore pressure can be estimated from the final equilibrium pressure, formation permeability, and borehole opening rate because pressure increases can occur if fluid is flowing into the borehole.

Permeability

In order to compare the pressure and flow response data measured at the fifteen boreholes, the data were interpreted to yield formation permeability. Permeability values were obtained assuming that the Salado Formation in the vicinity of each borehole could be modeled as a fully saturated, homogeneous, isotropic, porous medium. No attempts were made to interpret the data in terms of fracture flow, flow in a partially saturated porous medium, flow into a layered formation, or flow in a formation in which the permeability varies with radial distance from the borehole test region.

These estimations of permeability were derived from calculations based on measured parameters, with assumptions concerning the flow mechanisms that may not be valid for this formation. Nevertheless, they do provide a first-order approximation of permeability and a basis for additional research for determining flow mechanisms in the Salado. In particular, failure of the simple model to reproduce the measured results provides evidence that the data need to be examined in greater detail.

The time-dependent shut-in pressure response data typified by that shown on Figure 4 were analyzed using a modified version of a two-dimensional finite-element numerical code written by Wilson and Nickell [3]. This code is capable of simulating the borehole/packer/formation system geometries, borehole volume changes, and borehole storage effects including pressure dependent fluid compressibility which may occur if air bubbles are trapped in the test region. In addition, the permeability (k), porosity (ϕ), and viscosity (μ) may be input as functions of position, pressure, temperature and/or time. As a result, anisotropic permeabilities, borehole damage, non-darcy flow, and thermal effects can be considered, if desired. The code provides solutions to Equation 1

$$\beta \cdot \frac{\partial P}{\partial t} = \alpha \nabla^2 P + \frac{K_f\, w(t)}{\phi \rho} - \frac{K_f}{\phi V} \frac{\partial V}{\partial t} \qquad (1)$$

where P is the formation pressure, K_f is the fluid bulk modulus, ρ is the density, w(t) is a flow source or sink, and V is the appropriate test or guard region volume. β is defined in Equation 2

$$\beta = \left[1 - \frac{V_a}{\phi V} \frac{P_\infty}{P} + \frac{V_a}{\phi V} \frac{P_\infty}{P^2} K_f \right] \qquad (2)$$

where V_a is the volume of air trapped in the borehole as measured at a pressure P_∞, and the subscript ∞ denotes ambient conditions.

In the low permeability salt formations common to the WIPP, the matrix is assumed to be compressible with diffusivity, α, defined as shown in Equation 3.[4]

$$\alpha = \frac{k}{\mu} \left\{ C_m + \frac{\phi}{K_f} \right\}^{-1} \qquad (3)$$

with

$$C_m = \frac{1}{K + 4/3\, G} \qquad (4)$$

where G is the elastic shear modulus of the skeleton and K is the bulk modulus of the unsaturated or drained region.

For the low porosity salt formation, the first term in the brackets in Equation 3 is much larger than the second and, as a result, the flow is essentially independent of porosity and depends only on rock compressibility and permeability. In the results presented here, the diffusivity is as shown in Equation 5 as suggested by Nowak et al.[5]

$$\alpha = (1.1 \cdot 10^{14}) \cdot k \quad m^2/sec \qquad (5)$$

where k is given in units of m^2.

Permeability values are inferred from the measured data in an iterative manner using solutions to Equation 1. For example, a value is selected for the permeability and the pressure and time response is then calculated using the estimated pore pressure value and known borehole history. The measured and calculated responses are then compared. If they are similar, the permeability value is taken as representative of the formation. If they are not comparable, then a new permeability value is selected and the process repeated. Comparisons of some calculated and measured responses are shown on Figures 9-11. Note that throughout this report the terms pore pressure and formation pressure are used interchangeably.

The initial QPP03 pressure build-up is shown on Figure 9 to be consistent with the solid line that represents the calculated result for a formation having a poroelastic response with a $2.4 \cdot 10^{-10}$ darcy permeability and 12.8 MPa pore pressure. The pressure build-up that is observed after 35 days, when the test region pressure is lowered to 5.6 MPa and then shut-in, is much faster than predicted and corresponds to an approximate 10^{-9} darcy permeability. During the approximate 12 hour pressure build-up period, the pressure perturbance is estimated to have penetrated to a depth of about 4 cm from the borehole wall. This rapid pressure build-up is also consistently observed in tests where these packer systems have been set in lengths of casing; once the packers are set in the casing, it takes many hours for the test region pressure to equilibrate to a constant value. The observed rapid pressure build-up in the pulse test is therefore thought to occur because the test region volume is so small, and the associated test time is so short, that the response is dominated by the characteristics of the disturbed zone surrounding the borehole and/or system compliance effects. This rapid response is also observed in other borehole test region locations.

Results of three additional calculations are shown on Figure 10. They illustrate the sensitivity of the calculated pressure history to the selected permeability value, the length of time the borehole remained open prior to the initiation of the shut-in test, and the placement of a hypothetical 20 cc

air bubble in the vertically oriented QPP03 test region.

There are cases, as previously discussed, where the model only qualitatively reproduces the measured results. This is illustrated on Figure 11 where the calculated pressure response is compared to the measured QPP04 data. Even though this result is qualitative, it does suggest that the permeability is not significantly higher than $5.0 \cdot 10^{-21}$ darcy.

In a few tests, additional values of permeability were inferred from the approximately constant pressure data typified by that obtained during the late-time 20-50 day period shown on Figure 9. These analyses were performed so that comparisons could be made between the pre- and post-excavation responses. Post-excavation flow tests and subsequent pressure build-up tests have since been performed but this data has not yet been analyzed. Permeabilities were estimated from these data using Equation 6, a quasi-steady-state solution to Equation 1 for a cylindrical geometry

$$\frac{-\phi V}{K_f}\frac{dP_h}{dt} = 2\pi L \frac{K}{\mu}\frac{(P_h - P_o)}{\ln (R/r_h)} \qquad (6)$$

where L is the test region length, r is the radial distance measured from the center of the borehole, R is the maximum radial penetration of the pressure disturbance introduced by the test, and the subscripts h and o denote conditions at the borehole and radius R, respectively. For solutions of the diffusion equation (Equation 1), the $\ln(R/r_h)$ term is a function of the dimensionless time (τ_D) defined as $\alpha t/r_h^2$ as shown in Ferris et al. [8]. For larger values of τ_D, this term can be written as shown in Equation 7.

$$\ln (R/r_h) = 1/2 (\ln \tau_D + 0.80907) \qquad (7)$$

For the results given here, a value of 3.0 was used for this parameter. An order of magnitude increase in permeability only increases this dimensionless time quantity to 4.0.

The data from the 20 to 50 day period shown on Figure 9 corresponds to a 10^{-10} darcy permeability. This compares favorably to the $2 \cdot 10^{-10}$ darcy value determined using Equation 1 when evaluating the 0 to 30 day response.

RESULTS

The preliminary results as described in this section are divided into three areas of interest: 1) hydrologic characteristics of the undisturbed formation, 2) flow and pressure related phenomena that occurred during the mining process, and 3) excavation-induced changes in the local hydrologic characteristics.

Undisturbed Formation Characteristics

The hydrologic characteristics of the undisturbed formation are inferred from the results of the initial shut-in tests and the quasi-steady state responses observed prior to excavation of Room Q. Summaries of the measured pore pressures and permeabilities inferred from the data in the fifteen borehole test regions are presented in Tables 2 and 3.

The observed pressure responses generally fall into three categories which are related to the lithologic units. The interbed anhydrite regions that include Marker Bed 138 (QPP01), anhydrite "b" (QPP03), and Marker Bed 139 (QPP13) have 9 to 14 MPa pore pressures. Halite layers including Map Unit 7 (QPP04), that located below clay "d" (QPP12), and Map Unit 3 (QPP22, QPP23, QPP24, and QPP25) had lower pore pressures ranging from 5 to 10 MPa. The permeabilities in the halites in Map Unit 6 (QPP05), that below anhydrite "c" (QPP11), Map Unit 0 (QPP15), one location in Map Unit 3 (QPP21), and a polyhalitic halite layer (QPP14) were so low that pore pressure values could not be determined. In the halite of Map Unit 13 (QPP02), the test region pressure always equilibrated to an anomalously low 1.1 MPa value.

The shut-in pressures measured immediately prior to the excavation of Room Q are also shown in Table 2. These values are comparable to the listed pore pressures with the exception of borehole QPP23, which was discussed previously.

Permeability values are given in Table 3 for the 15 borehole test regions. These values were determined from initial pressure build-up data similar to that shown on Figure 9 for QPP03. The fourth column shows permeability values calculated from pressure data only, while the results shown in the fifth column were obtained using both pressure and diameter change data. The analysis determines a product (kh) of the permeability (k) and flow layer thickness (h). Permeability values in Table 3 were calculated by assuming a thickness equal to the test region length. For the interbed regions, this assumption may not be valid and the permeability values obtained should be adjusted once the interbed thicknesses are determined.

If pressure data alone are considered, the permeabilities determined from boreholes having measurable pore pressures are less than about one nanodarcy. A permeability value could not be determined from QPP02 data.

Even if the borehole deformation effects are considered, the permeability values remained less than about two nanodarcies. Since there was no significant pressure rise during the QPP05 shut-in test, the borehole deformation results suggest that the borehole volume increase and brine inflow rates were equivalent. The permeability value shown on Table 3 for QPP05 was estimated by assuming an 8.0 MPa pore pressure, similar to that measured for QPP22, QPP23, QPP24, and QPP25.

Inclusion of borehole deformation effects significantly changes the permeabilities estimated from QPP05, QPP12, QPP13, and QPP22 borehole data. For example, a 3.8 cm borehole closing at a rate of 40 μstrains/day would have an initial pressure rise equivalent to that seen on Figure 9 for QPP03 provided that the formation is impermeable. The

fact that many borehole diameters, and therefore volumes, are apparently increasing is not understood. As a result, work is continuing to determine the reliability and accuracy of the borehole deformation data. Subsequent to the tests reported here, the test region pressures were lowered to less than 1 MPa. At these lower pressures, closure was observed in all the 10.2 cm diameter boreholes but in only a few of the 3.8 cm diameter boreholes.

The pre-excavation normalized (average for the two orthogonal gages) borehole diameter change rates are listed in the sixth column of Table 3. Borehole diameters are seen to change at normalized rates ranging between -4 and 63 microstrains/day with a positive change rate indicating that the hole is opening. The gages in the 10.2 cm diameter boreholes, QPP01, QPP11, and QPP21, have 48 cm long by 10 cm wide platens that contact the borehole wall. The deformation gages in the 3.8 cm boreholes have 0.6 cm diameter pin contacts. The larger diameter gages did measure hole closure successfully on earlier tests. The tests examined in this report mark the first attempt to use the small diameter gages.

Excavation Response

During the excavation process, the borehole pressures were maintained at sufficiently low values so that fracturing would not occur if the local stresses decreased. As a result, the quantity of information available to describe the dynamic response associated with the excavation of the room is limited.

The effect of the excavation on borehole diameter change rates, test region pressures, and test region brine inflow rates, are shown in Figures 12 through 15. Note that while a full set of data exists for each borehole, these figures were chosen to best represent the effects of excavation on these parameters. Excavation history data are superimposed on these figures to show the temporal relationship between the mining process and responses within a particular test region. (Note on Figures 12 through 15 this is illustrated by the solid line labeled "Excavation Progress" for which each vertical step increment represents the mining of that proportionate length of the 110 m long room.) As shown on these figures, timing of the excavation-induced formation response is nearly the same for all test locations including the near-excavation test regions such as QPP15 and the outer-most test regions such as QPP21.

Perturbation of the surrounding formation as a result of excavation is illustrated most dramatically by the borehole deformation data. Examination of Figure 12 reveals that the step-like changes in diameter are coincident with the advances of the boring machine. Note that the most dramatic step occurs as the cutter head passed the gage locations. These step-like responses were sometimes followed by gradual borehole diameter changes that may have continued for three or four days. The diameter changes at all locations are qualitatively similar, and in general, the magnitudes of the responses decreased with increasing distance from the excavation.

Three significant observations can be made based on the borehole diameter change measurements. First, diameter changes in the hoop direction, oriented relative to Room Q, are in general larger than those in the radial direction. Second, the diameters in both the hoop and radial directions generally decreased as a result of the excavation of Room Q. Finally, the measured borehole to borehole diameter changes do not vary uniformly with distance from Room Q. For a hole aligned with the Room Q axis, the measured diameters are in the vertical and horizontal directions. The measured diameters do not align exactly in the hoop and radial directions because the boreholes slant with respect to the Room Q axis as shown on Figure 1.

Typical shut-in pressure data are shown on Figures 13 and 14. Borehole QPP21 experienced a 0.6 MPa pressure increase and borehole QPP02 a 0.7 MPa pressure excursion during the period between 83 and 100 days. As with the borehole deformation measurements, the data reflect the discrete mining steps.

Figure 15 shows measured changes in the QPP23 test region brine reservoir volume during excavation of Room Q. During this period, the brine reservoir was used to maintain the test region pressure at approximately 3.5 MPa. Again, the discrete advances of the boring machine are reflected in the flow data. A maximum change in the accumulator brine volume of 4.4 cc occurs nearly coincident with the boring machine passing the gage location. During this time, the corresponding decrease in borehole diameter equates to a 3.8 cc reduction in test region volume.

A typical temperature response is shown in Figure 16. The temperature increased at borehole QPP03 approximately two days after the boring machine passed the gage location. A delay in temperature arrival of this magnitude is consistent with an approximate 0.03 cm^2/sec thermal diffusivity for salt. There were no measured temperature changes at the boreholes located 4.2 room diameters outside the excavation. Clearly, the rapid responses described in the preceding paragraphs are not the result of thermal loads induced by the mining process.

Post-Excavation Formation Characteristics

Post-excavation hydrologic characteristics are inferred primarily from the steady state shut-in test response data typical of that shown on Figures 17 and 18. The pre- and post-excavation results are compared in Tables 4, 5, and 6.

Measured pre- and post-excavation shut-in pressures are compared in Table 4. Two of the three anhydrite interbed regions showed excavation-induced changes in shut-in pressure with those in anhydrite "b" (QPP03) and Marker Bed 139 (QPP13) decreasing by 4.7 and 2.7 MPa, respectively. The Marker Bed 138 (QPP01) shut-in pressure remained relatively unchanged.

The halite layers tested using boreholes QPP04, QPP12, QPP22, QPP23, QPP24, and QPP25 that had pre-excavation shut-in pressures between 3.6 and 9.1

MPa showed varied responses. As shown on Table 4, the pressures either remained approximately constant or decreased. The most noticeable decreases occurred in boreholes QPP24 and QPP25, which are positioned close to the room.

Pre-excavation shut-in pressures could not be measured in the halite layers tested using boreholes QPP05, QPP11, QPP14, QPP15, and QPP21. All of these layers had measurable post-excavation shut-in pressures. The shut-in pressure in Map Unit 13 (QPP02) that had the anomalously low pre-excavation 1.1 MPA value increased to 1.2 MPa following excavation of the room.

Post-excavation shut-in pressures were measured in all 15 test locations. Of these, 12 showed effects of the excavation. This is true not only of the test regions located near the excavation, but also in the test regions located 4.2 room diameters outside the room.

In a few cases, Equation 6 could be used to determine permeability values from the 20-50 day shut-in pressure data typical of that shown on Figure 10. These results are compared with similarly determined post-excavation values in Table 5. Since the post-excavation pore pressures are inferred from the shut-in pressure data, the Table 5 values must be considered as qualitative. Although there is some indication that the permeabilities may have changed, the estimated pre- and post-excavation values are generally similar to the permeability changes that could result from changes in the borehole deformation rate. There is no clear indication that permeability values significantly increased as a result of the excavation of Room Q.

The pre- and post-excavation normalized borehole diameter change rates are compared in Table 6. Prior to the excavation, the borehole diameters changed at rates ranging between -4 and 63 microstrains/day where the positive sign indicates a borehole is opening. Following excavation of the room, the diameters changed at rates ranging between -42 and 48 microstrains/day. Examination of the data shows that the Room Q excavation influences the response even out to the farthest test regions.

CONCLUSIONS

Prior to excavating Room Q, the data indicate that the undisturbed formation had the following characteristics:

1. The three interbed regions tested had 9-14 MPa pore pressures. Three halite layers with measurable pore pressures had 7-10 MPa values and one anomalous layer had a 1.1 MPa value. Five halite regions had permeabilities that were so low that the pore pressures could not be determined.

2. In all but one of the regions having measurable pore pressures tested, the permeabilities, as inferred from shut-in tests, were less than two nanodarcies. A permeability value could not be determined from the data obtained in the halite layer that had the anamolously low pore pressure. One region had a permeability of approximately ten nanodarcies.

3. The normalized test region borehole diameter change rates ranged between -4 and 63 microstrains/day. At this time we cannot explain why the borehole diameters, and therefore volumes, were apparently increasing rather than decreasing.

During the excavation period:

4. All pressure, flow, and borehole diameter change data show step-like changes coincident with the advances of the boring machine.

5. The shut-in pressure, flow and borehole diameter changes at all locations are qualitatively similar with the magnitudes of the response generally decreasing with increasing distance from the rib.

6. Test region borehole diameter changes in the hoop direction, oriented relative to Room Q, are generally larger than those in the radial direction. However, both diameters generally decreased during the excavation process.

7. The onset of the excavation-induced temperature rise at the test regions is consistent with an approximate 0.03 cm^2/sec thermal diffusivity for salt. The responses described in conclusions 4 and 5 clearly does not result from thermal loading induced by the excavation process.

The shut-in pressure tests were continued following excavation of Room Q. However, because sufficient data have not yet been analyzed, a definitive description of the long term changes in the hydrologic response cannot be provided at this time. Consequently, the following observations are qualitative and preliminary:

8. At 12 of the 14 locations, post-excavation shut-in pressure differed from pre-excavation values. This effect was observed even at the outer-most test regions located 4.2 room diameters outside the rib.

9. Post-excavation shut-in pressures could be measured in all the halite layers that had low pre-excavation permeabilities which prevented definitive pre-excavation formation pressures from being measured.

10. In the cases where post-excavation and pre-excavation permeabilities in a specific borehole could be qualitatively estimated, the results were comparable.

11. The pre- and post-excavation borehole diameter change rates were different for nine of the fourteen test regions with definitive data. In general, the rates of opening decreased.

In summary, prior to the excavation of Room Q, the inferred formation pore pressures ranged between 1 and 14 MPa and the associated permeabilities were

less than one nanodarcy. The flow properties of the Salado Formation are very heterogeneous. Each interbed region had its own unique set of characteristics as did each of the tested halite regions.

The excavation of Room Q affected the formation response at the outer-most boreholes located 4.2 room-diameters from the excavation. The effects appeared immediately and are coincident with advances of the boring machine. The magnitude of the change generally decreased with increasing distance from the rib, however, the responses cannot be considered uniform. In those regions where pre-excavation shut-in pressures could be measured, post-excavation values were generally lower. Following excavation of Room Q, shut-in pressures could also be measured in the halite layers that had pre-excavation permeabilities that were so low that they precluded such measurements. In general, there was no clear indication that the overall magnitude of formation permeability was significantly increased after the excavation of Room Q.

ACKNOWLEDGMENTS

We would like to thank the Sandia, S-Cubed, Re/Spec, and Westinghouse field crews, especially Cliff Howard of Re/Spec, for their efforts in excavating Room Q, drilling the boreholes, installing the packer system and monitoring equipment, and continued maintenance of the test systems. This work was sponsored by the U.S. Department of Energy under contract number DE-AC04-76DP00789.

REFERENCES

1. Horner, D. R.: "Pressure Build-Up in Wells," Proceedings, Third World Petroleum Congress, The Hague (1951) Section II, 503- 523, Pressure Analysis Methods, SPE Reprint Series, Society of Petroleum Engineers, Dallas (1967) 9, 25-43.

2. Ehlig-Economides, C. A. and Ramey, H. J., Jr.,: "Pressure Build-Up for Wells Produced at Constant Pressure," Society of Petroleum Engineers Journal (February 1981), 105-114.

3. Wilson, E. L. and Nickell, R. E.: "Application of the Finite Element Method to Heat Conduction Analysis," Nuclear Engineering and Design 4 (1966) 276-286, North-Holland Publishing Company, Amsterdam.

4. Garg, S. K.: "On Diffusivity Equations for Liquid-Saturated Porous Media Reservoirs," Energy Sources, Vol. 9, pp. 261-268, 1987.

5. Nowak, E. J., McTigue, D. F., and Beraun, R.: "Brine Inflow to WIPP Disposal Rooms: Data, Modeling, and Assessment," Sandia National Report, SAND88-0112, September 1988.

6. Ferris, J. G., Knowles, D. B., Brown, R. H., and Stallman, R. W.: "Theory of Aquifer Tests," U. S. Geological Survey Water-Supply Paper 1536-E, 1962.

Table 1. Room Q pressure/flow/closure system test configurations.

BOREHOLE	BOREHOLE DIA/DEPTH (cm) / (m) [4]	TOOL TYPE	TEST REGION LENGTH (cm) [1]	TEST REGION VOLUME (cc) [2]	GUARD REGION LENGTH (cm) [3]	GUARD REGION VOLUME (cc) [2]
QPP01	10 / 13.7	DUAL	188	5.1×10^3	76	2.0×10^3
QPP02	3.8 / 7.6	SINGLE	85	290	--	--
QPP03	3.8 / 4.6	DUAL	90	300	14	135 [5]
QPP04	3.8 / 3.4	SINGLE	85	290	--	--
QPP05	3.8 / 2.4	DUAL	90	300	14	135
QPP11	10 / 13.7	DUAL	135	6.0×10^3	76	2.0×10^3
QPP12	3.8 / 7.6	SINGLE	85	290	--	--
QPP13	3.8 / 4.6	DUAL	90	300	14	135
QPP14	3.8 / 3.4	SINGLE	85	290	--	--
QPP15	3.8 / 2.4	DUAL	90	300	14	135
QPP21	10 / 13.7	DUAL	135	6.1×10^3	76	2.0×10^3
QPP22	3.8 / 7.6	SINGLE	85	290	--	--
QPP23	3.8 / 4.6	DUAL	90	300	14	135
QPP24	3.8 / 3.4	SINGLE	85	290	--	--
QPP25	3.8 / 2.4	DUAL	90	300	14	135

NOTES:

1. The test region extends from the bottom of the hole to the wellbore contact of the deepest packer.
2. The test and guard region volumes include the volume of the connecting lines.
3. The guard region lengths are the distances between the wellbore contacts of the two packers. The distances between the test and guard regions are 33 cm (3.8 cm dia. hole) and 25 cm (10 cm dia. hole).
4. This depth is measured radially from the centerline of Room Q.
5. The test and guard regions were combined (*i.e.*, the test region packer failed) to give a 137 cm long, 435 cc test region.

Table 2. Summaries of the estimated undisturbed far-field pore pressures determined from the initial shut-in test and the actual shut-in pressure measured just prior to excavation of Room Q.

BOREHOLE	LOCATION[1]		FAR-FIELD PORE PRESSURE (MPa)	PRE-EXCAVATION SHUT-IN PRESSURE (MPa)
	VERT (m)	HORIZ (m)		
QPP01	13.7	0	9.3 - 13.9	9.3
QPP02	7.6	0	1.1	1.1
QPP03	4.6	0	12.8	11.5
QPP04	3.4	0	7.0 - 10.3	7.0
QPP05	2.4	0	--- [2]	-- [2]
QPP11	-13.7	0	--- [2]	-- [2]
QPP12	-7.6	0	5.8 - 8.6	5.8
QPP13	-4.6	0	10.7 - 12.8	10.5
QPP14	-3.4	0	--- [2]	-- [2]
QPP15	-2.4	0	--- [2]	-- [2]
QPP21	0	13.7	--- [2]	-- [2]
QPP22	0	7.6	9.1 - ?	8.5
QPP23	0	4.6	7.3 - 9.4	3.6
QPP24	0	3.4	9.1 - ?	6.3
QPP25	0	2.4	7.7 - 9.1	7.7

NOTES:

1. The location is measured with respect to the Room Q centerline.
2. Indicates formation held pressure at arbitrary set value.

Table 3. Summary of the undisturbed far-field permeabilities determined from the initial shut-in and borehole deformation data.

BOREHOLE	LOCATION [1]		INITIAL SHUT-IN TEST PERMEABILITY (darcy)		NORMALIZED DIAMETER CHANGE RATE (μ Strains/day)
	VERT (m)	HORIZ (m)	PRESSURE DATA ONLY	PRESSURE AND DIAMETER CHANGE DATA	
QPP01	13.7	0	1.5×10^{-9}	2.3×10^{-9}	17
QPP02	7.6	0	[4]		35
QPP03	4.6	0	2.4×10^{-10}		-4
QPP04	3.4	0	5.0×10^{-11}		7
QPP05	2.4	0	[2]	2×10^{-10} [3]	19
QPP11	-13.7	0	[2]		0
QPP12	-7.6	0	2×10^{-11}	2×10^{-10}	24
QPP13	-4.6	0	3×10^{-10}	2×10^{-9}	63
QPP14	-3.4	0	[2]		0
QPP15	-2.4	0	[2]		22
QPP21	0	13.7	[2]		0
QPP22	0	7.6	1×10^{-10}	5×10^{-10}	23
QPP23	0	4.6	1×10^{-9}	1.5×10^{-9}	7
QPP24	0	3.4	1×10^{-9}	1.5×10^{-9}	17
QPP25	0	2.4	1×10^{-10}		0

NOTES:

1. The location is measured with respect to the Room Q centerline.
2. Permeability is too low to measure.
3. The pore-pressure was arbitrarily selected at 8.0 MPa in order to determine a permeability from the diameter change data.
4. Indicates that results are indeterminate.

Table 4. Comparison of the pre- and post-excavation measured shut-in pressures.

BOREHOLE	LOCATION[1]		PRE-EXCAVATION SHUT-IN PRESSURE (MPa)	POST-EXCAVATION SHUT-IN PRESSURE (MPa)	RESPONSE CHANGED BY EXCAVATION	COMMENTS
	VERT (m)	HORIZ (m)				
QPP01	13.7	0	9.3	10.1	no	–
QPP02	7.6	0	1.1	1.2	yes	–
QPP03	4.6	0	11.5	6.8	yes	–
QPP04	3.4	0	7.0	6.5	yes	Pre-excavation value was slowly increasing.
QPP05	2.4	0	(2)	0.5	yes	–
QPP11	-13.7	0	(2)	5.0	yes	Post-excavation value continuing to increase.
QPP12	-7.6	0	5.8	8.5	no	Pre-excavation value was slowly increasing.
QPP13	-4.6	0	10.5	7.8	yes	–
QPP14	-3.4	0	(2)	5.9	yes	–
QPP15	-2.4	0	(2)	2.4	yes	Post-excavation value continuing to increase.
QPP21	0	13.7	(2)	4.7	yes	–
QPP22	0	7.6	1	8.5	yes	Pre-excavation value was increasing.
QPP23	0	4.6		3.6	?	Pre-excavation value decreasing.
QPP24	0	3.4	6.3	2.5	yes	Post-excavation value increasing.
QPP25	0	2.4	7.7	3.0	yes	–

NOTES:

1. The location is measured with respect to the Room Q centerline.
2. Indicates formation held pressure at arbitrary set value.

Table 5. Comparison of the pre- and post-excavation permeability values determined from the shut-in data using *Eq.* (6).

BOREHOLE	LOCATION [1]		PRE-EXCAVATION PERMEABILITY (darcy)	POST-EXCAVATION PERMEABILITY (darcy)
	VERT (m)	HORIZ (m)		
QPP01	13.7	0	4×10^{-9} [2]	2×10^{-9} [2]
QPP02	7.6	0	[3]	[3]
QPP03	4.6	0	1×10^{-10}	1×10^{-10}
QPP04	3.4	0	5×10^{-11}	[3]
QPP05	2.4	0	2×10^{-10} [2]	[3]
QPP11	-13.7	0	[3]	[3]
QPP12	-7.6	0	3×10^{-10} [2]	5×10^{-10} [2]
QPP13	-4.6	0	2×10^{-9} [2]	1×10^{-9} [2]
QPP14	-3.4	0	[3]	6×10^{-10} [2]
QPP15	-2.4	0	[3]	[3]
QPP21	0	13.7	[3]	[3]
QPP22	0	7.6	[3]	[3]
QPP23	0	4.6	[3]	[3]
QPP24	0	3.4	[3]	[3]
QPP25	0	2.4	[3]	[3]

NOTES:

1. The location is measured with respect to the Room Q centerline.
2. Corrected for borehole diameter change.
3. Indicates results are indeterminate.

Table 6. Comparison of the pre- and post-excavation normalized borehole diameter change rates.

BOREHOLE	LOCATION[1]		NORMALIZED[2] PRE-EXCAVATION DIAMETER CHANGE RATE (μ Strain/day)	NORMALIZED[2] POST-EXCAVATION DIAMETER CHANGE RATE (μ Strain/day)	RESPONSE CHANGED BY EXCAVATION
	VERT (m)	HORIZ (m)			
QPP01	13.7	0	17	2	yes
QPP02	7.6	0	35	no data	--
QPP03	4.6	0	-4[3]	0	yes
QPP04	3.4	0	7[3]	25	yes
QPP05	2.4	0	19	-42[3]	yes
QPP11	-13.7	0	0	-1	no
QPP12	-7.6	0	24	24	no
QPP13	-4.6	0	63	48	no
QPP14	-3.4	0	0	17	yes
QPP15	-2.4	0	22	16	yes
QPP21	0	13.7	0	-1	no
QPP22	0	7.6	23	27	no
QPP23	0	4.6	7	2[3]	yes
QPP24	0	3.4	17	-9[3]	yes
QPP25	0	2.4	0	8[3]	yes

NOTES:

1. The location is measured with respect to the Room Q centerline.
2. Values shown represent the average change rate for the two closure gauges, normalized to the borehole diameter.
3. Indicates one diameter is increasing and one diameter is decreasing.

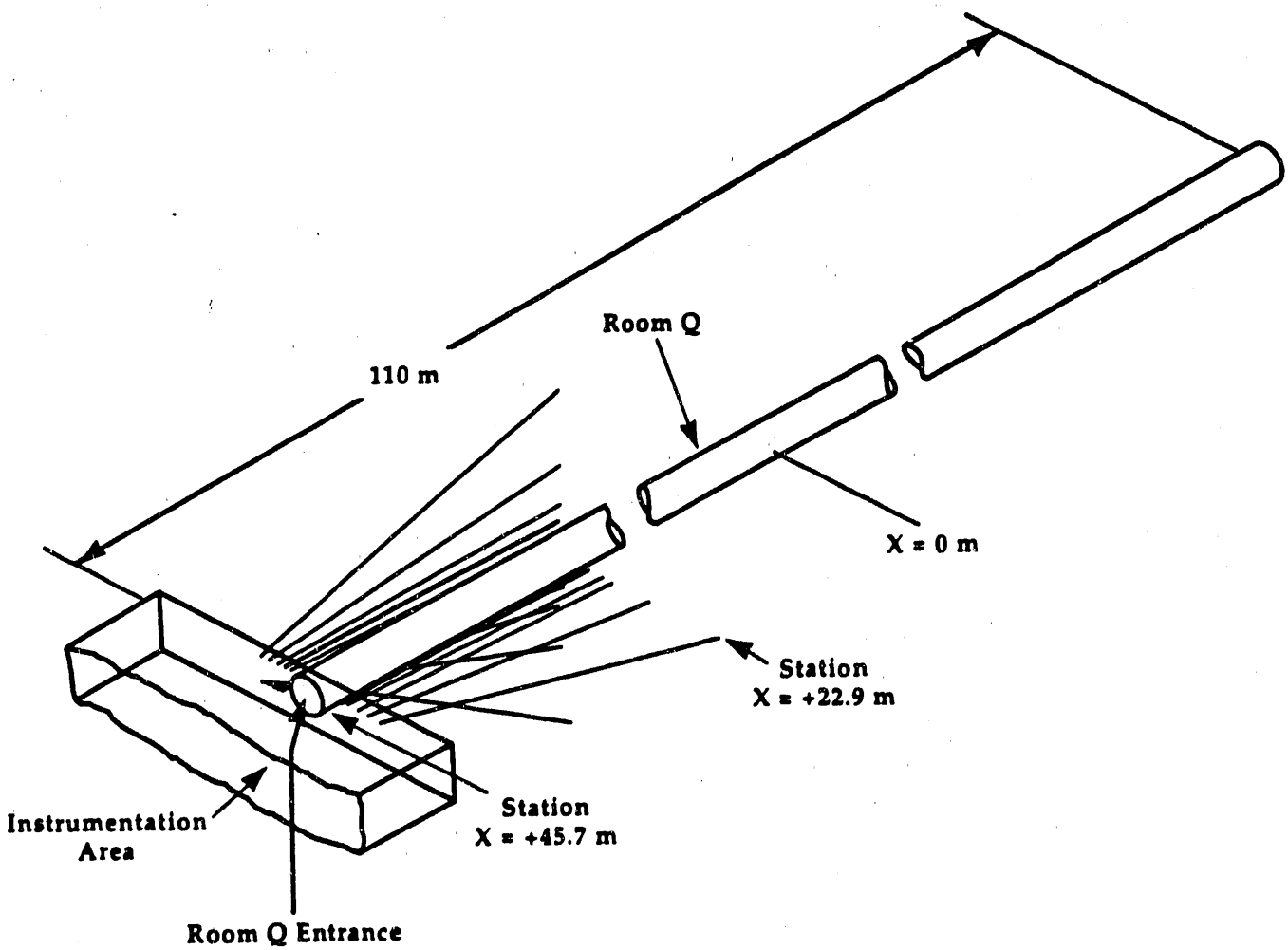

Figure 1. Room Q pressure/flow/closure system test locations.

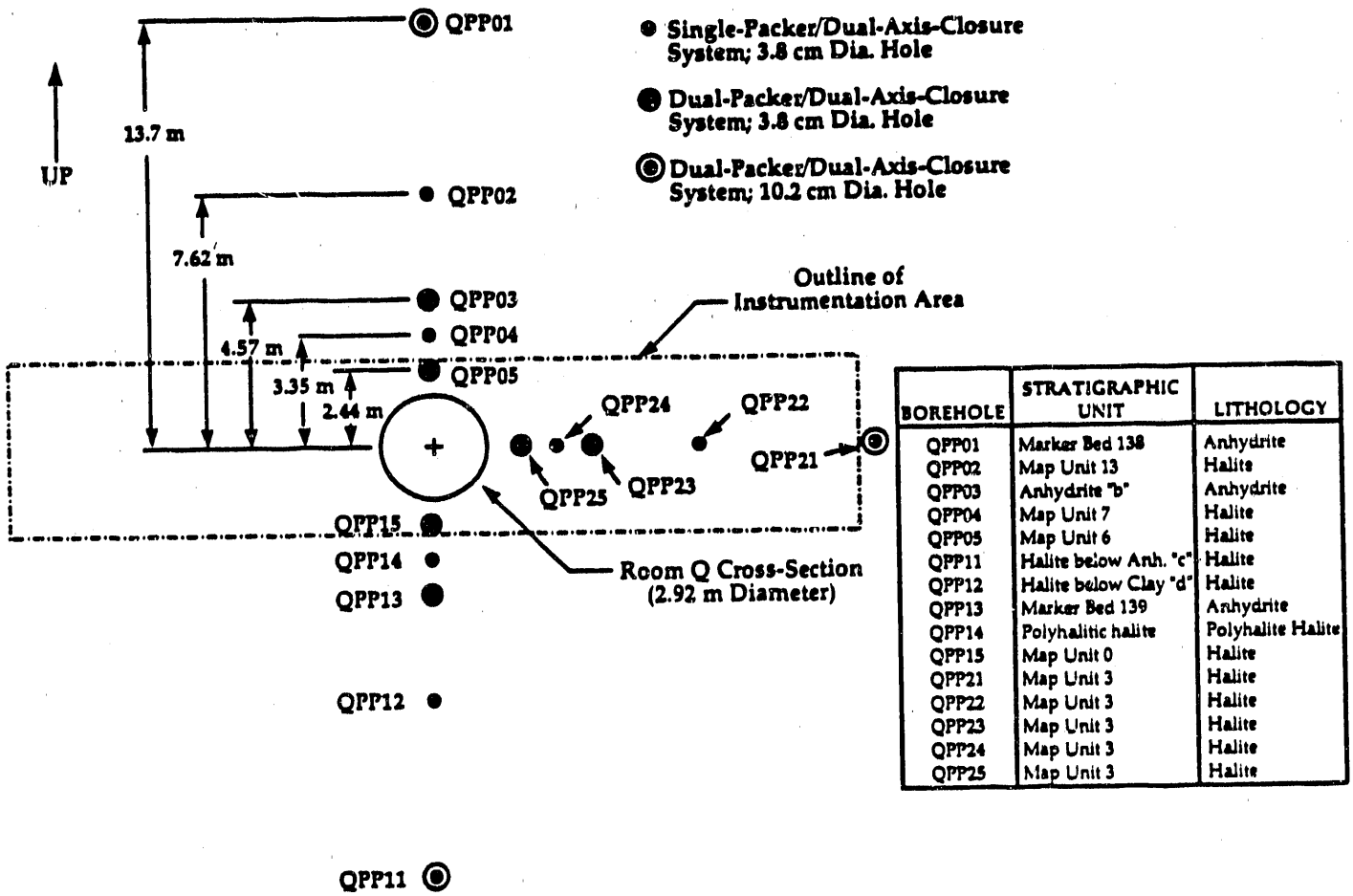

BOREHOLE	STRATIGRAPHIC UNIT	LITHOLOGY
QPP01	Marker Bed 138	Anhydrite
QPP02	Map Unit 13	Halite
QPP03	Anhydrite "b"	Anhydrite
QPP04	Map Unit 7	Halite
QPP05	Map Unit 6	Halite
QPP11	Halite below Anh. "c"	Halite
QPP12	Halite below Clay "d"	Halite
QPP13	Marker Bed 139	Anhydrite
QPP14	Polyhalitic halite	Polyhalite Halite
QPP15	Map Unit 0	Halite
QPP21	Map Unit 3	Halite
QPP22	Map Unit 3	Halite
QPP23	Map Unit 3	Halite
QPP24	Map Unit 3	Halite
QPP25	Map Unit 3	Halite

Figure 2. Radial positions of the pressure/flow/closure measurement systems.

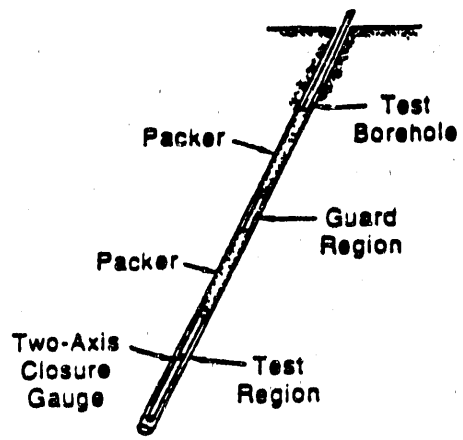

a) Dual-Packer/Closure Gauge Assembly

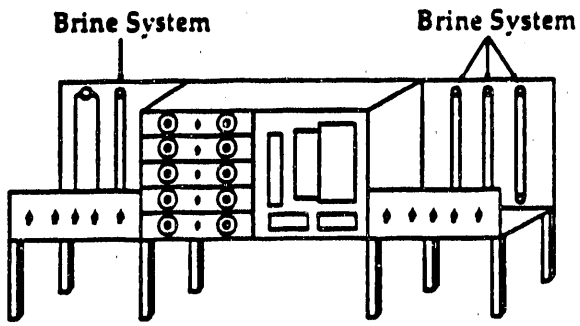

b) Flow-Control/Data Acquisition Cabinet

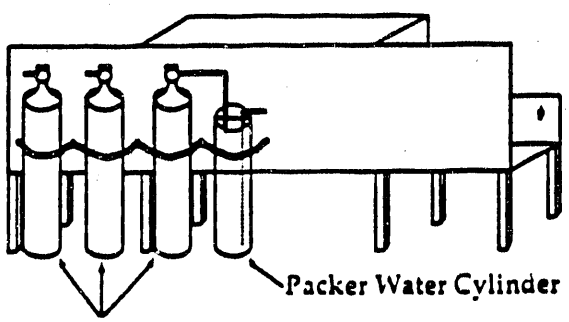

c) Pressurized Cylinders Attached to Cabinet

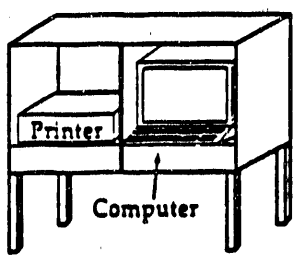

d) Computer/Printer Cabinet

Figure 3. Schematic diagrams of the borehole pressure/flow/closure measurement system.

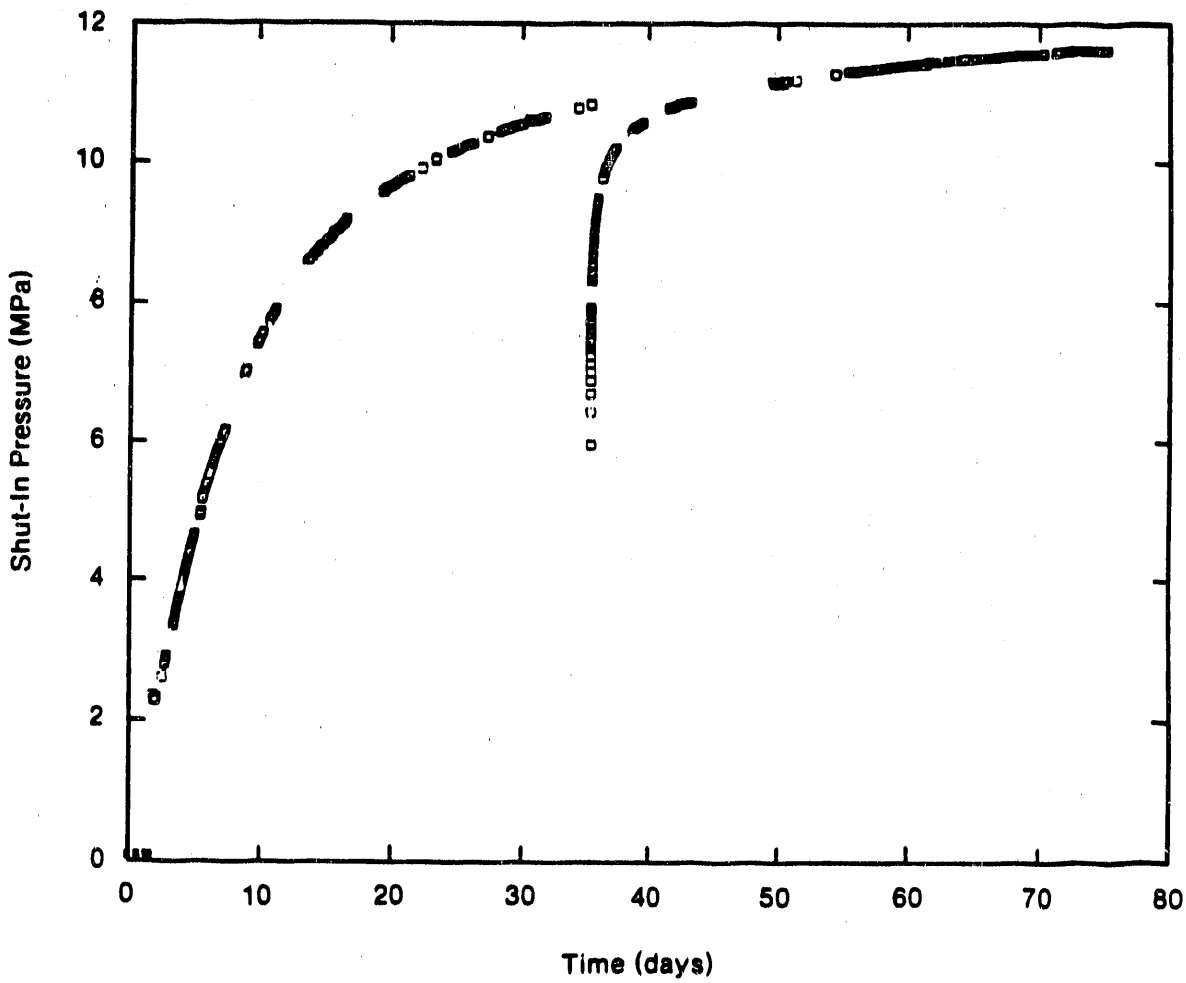

Figure 4. QPP03 test region shut-in pressure.

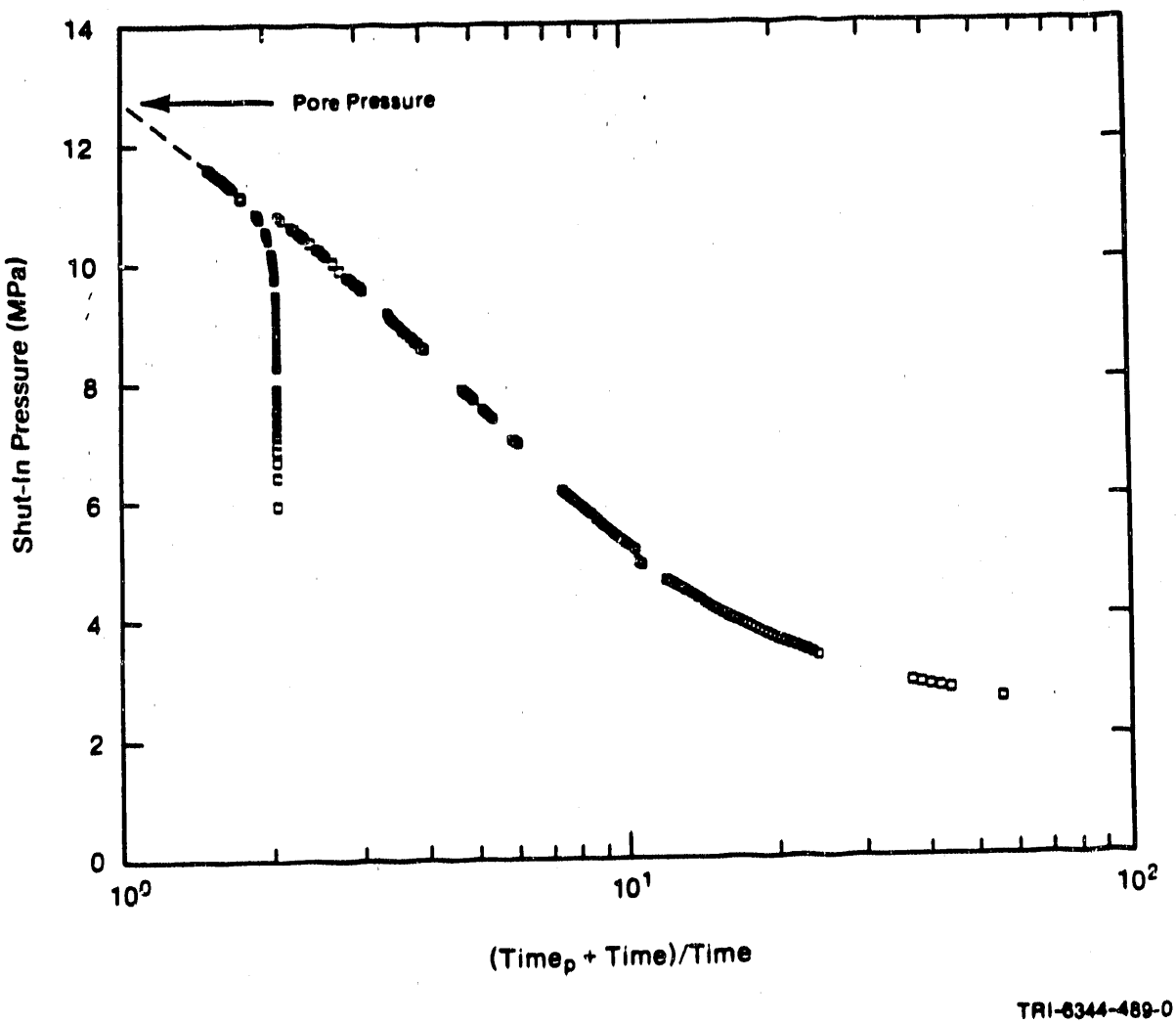

Figure 5. Horner-like plot of the QPP03 shut-in pressure data.

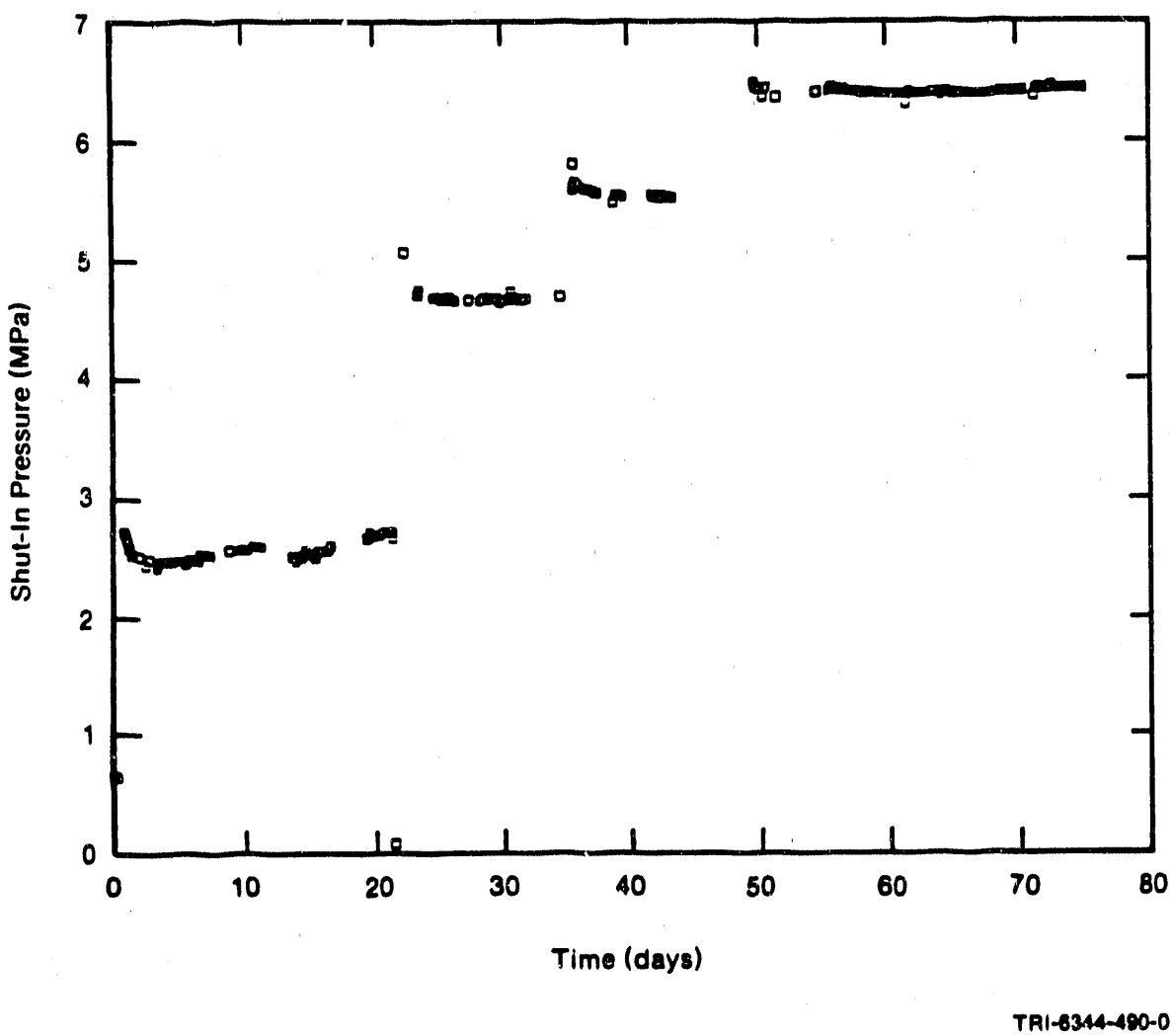

Figure 6. QPP15 test region shut-in pressure response.

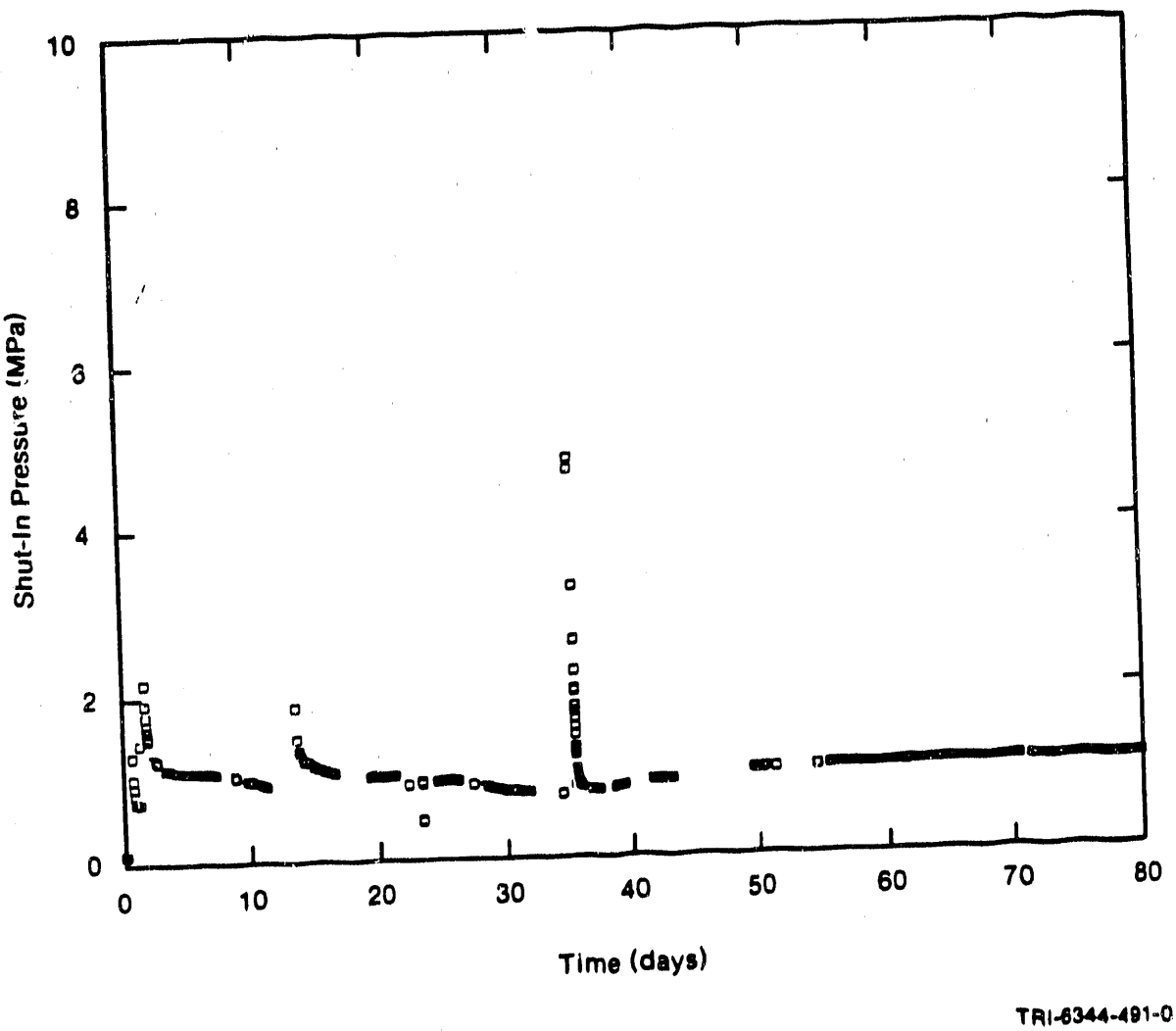

Figure 7. QPP02 test region shut-in pressure.

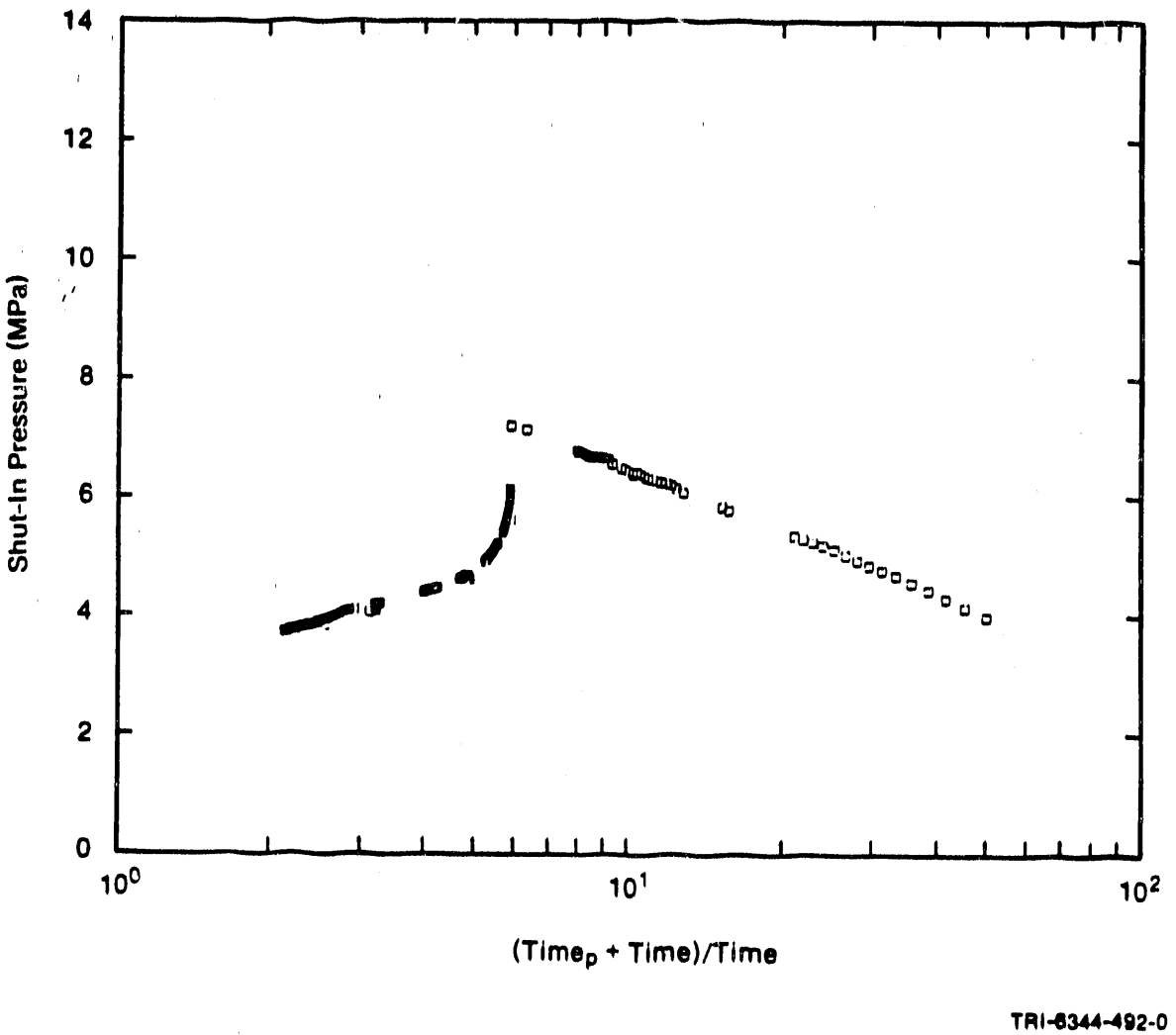

Figure 8. Horner-like plot of the QPP23 shut-in pressure data.

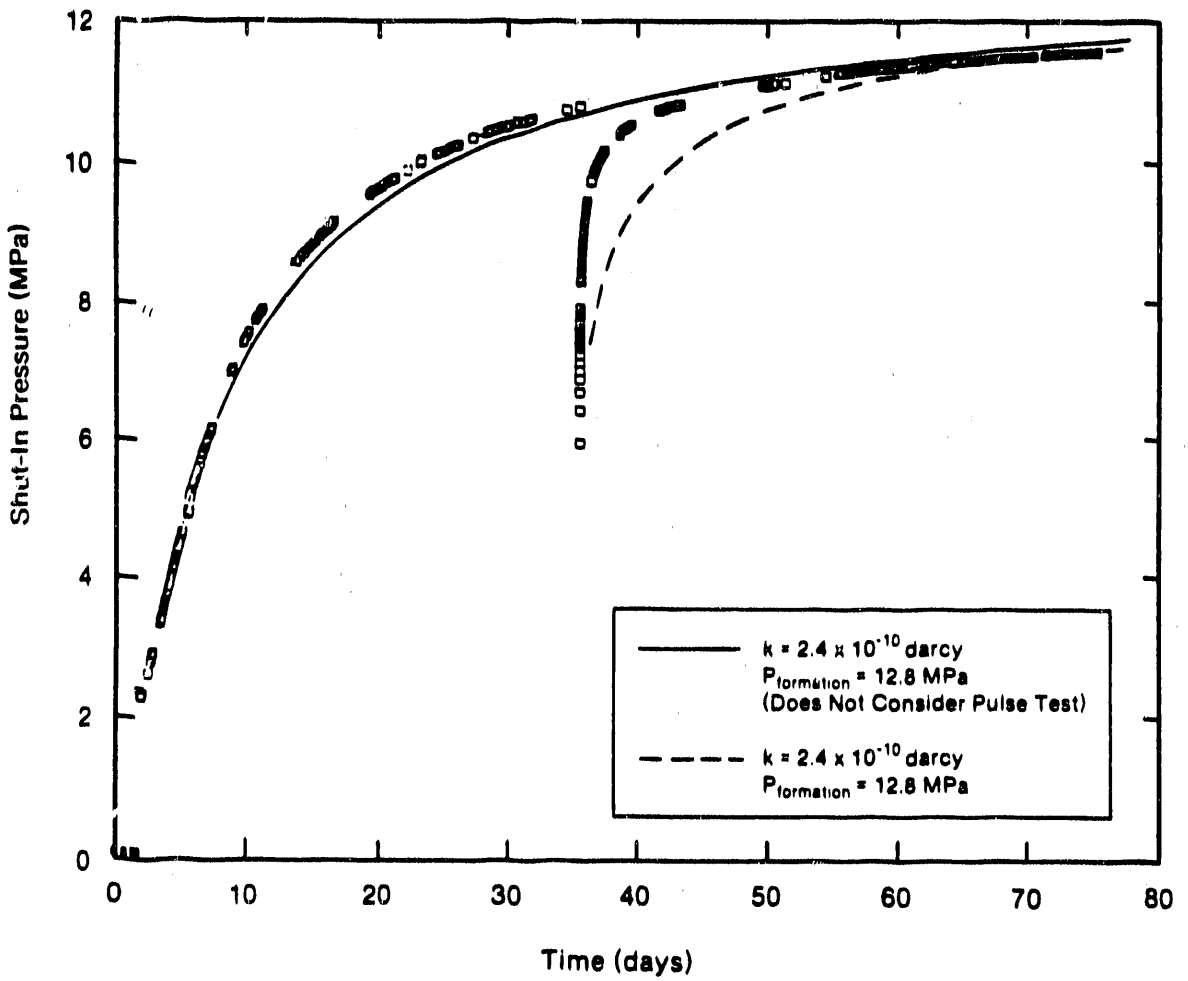

TRI-6344-493-0

Figure 9. Comparison of the measured and calculated QPP03 test region shut-in pressure response.

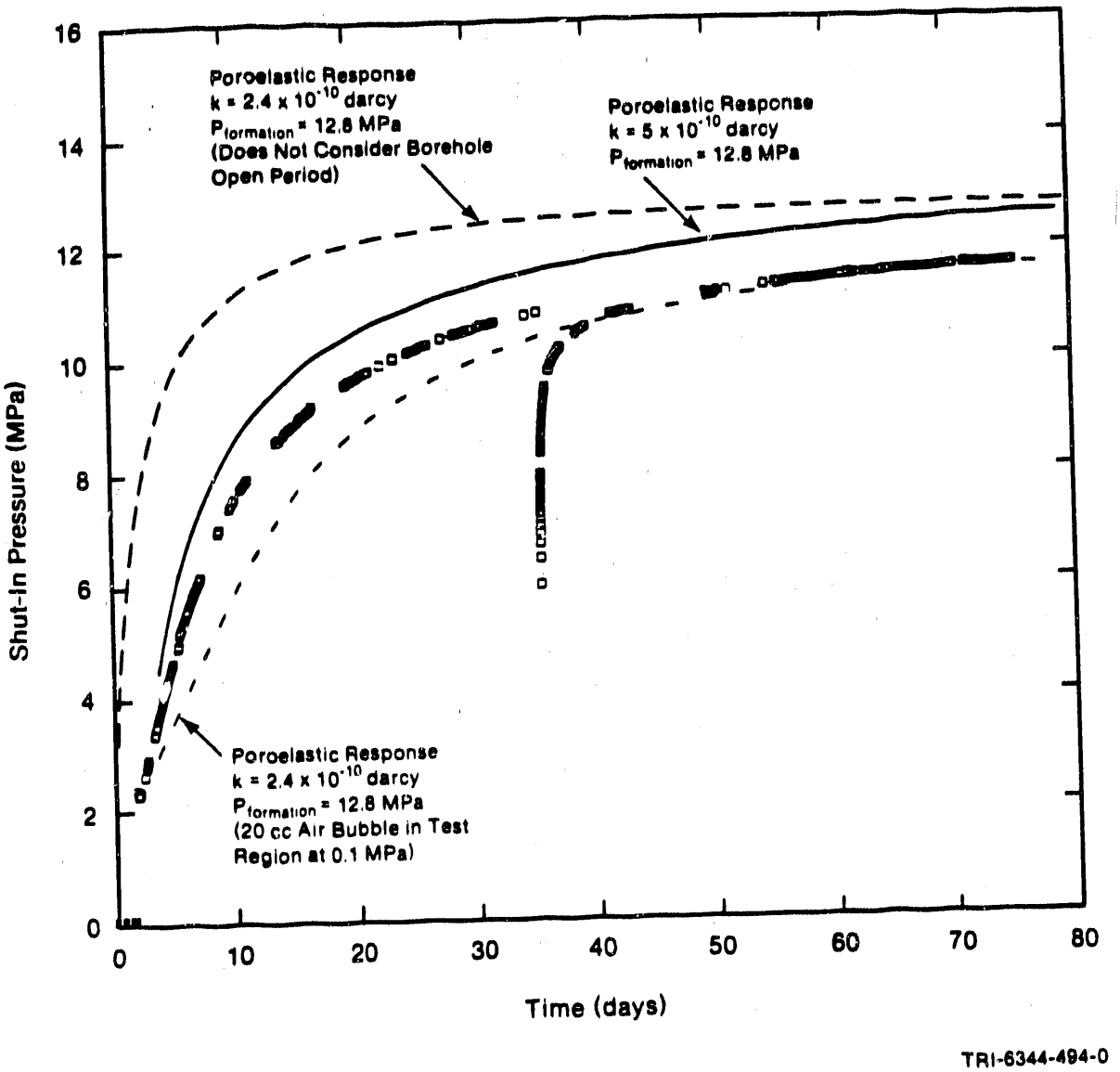

Figure 10. Comparison of the measured and calculated QPP03 test region shut-in pressure responses showing the effects of the borehole open period, a 0.5 nanodarcy permeability, and an air bubble in the test region.

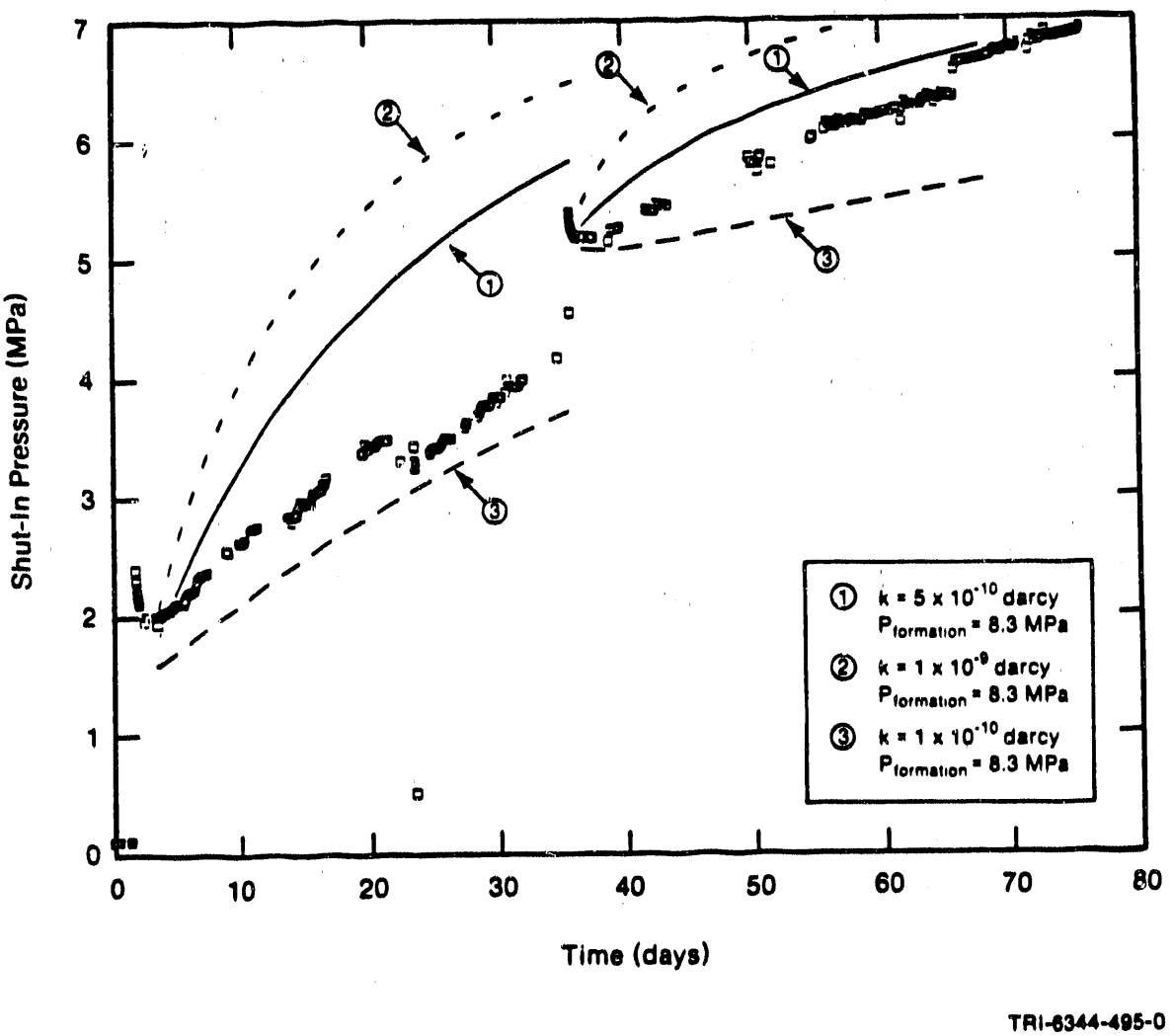

TRI-6344-495-0

Figure 11. Comparison of the measured and calculated QPP04 test region shut-in pressure responses.

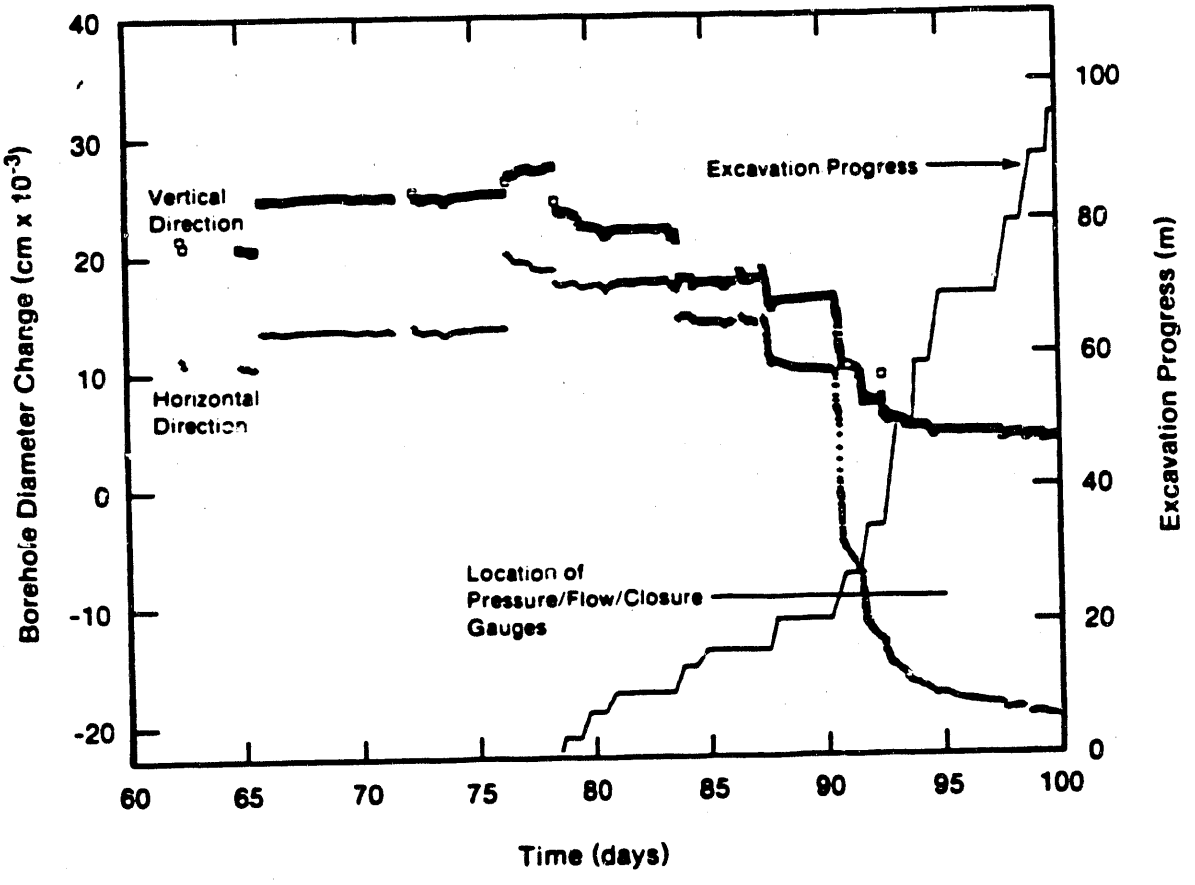

Figure 12. Borehole diameter changes measured on QPP15 during excavation of Room Q.

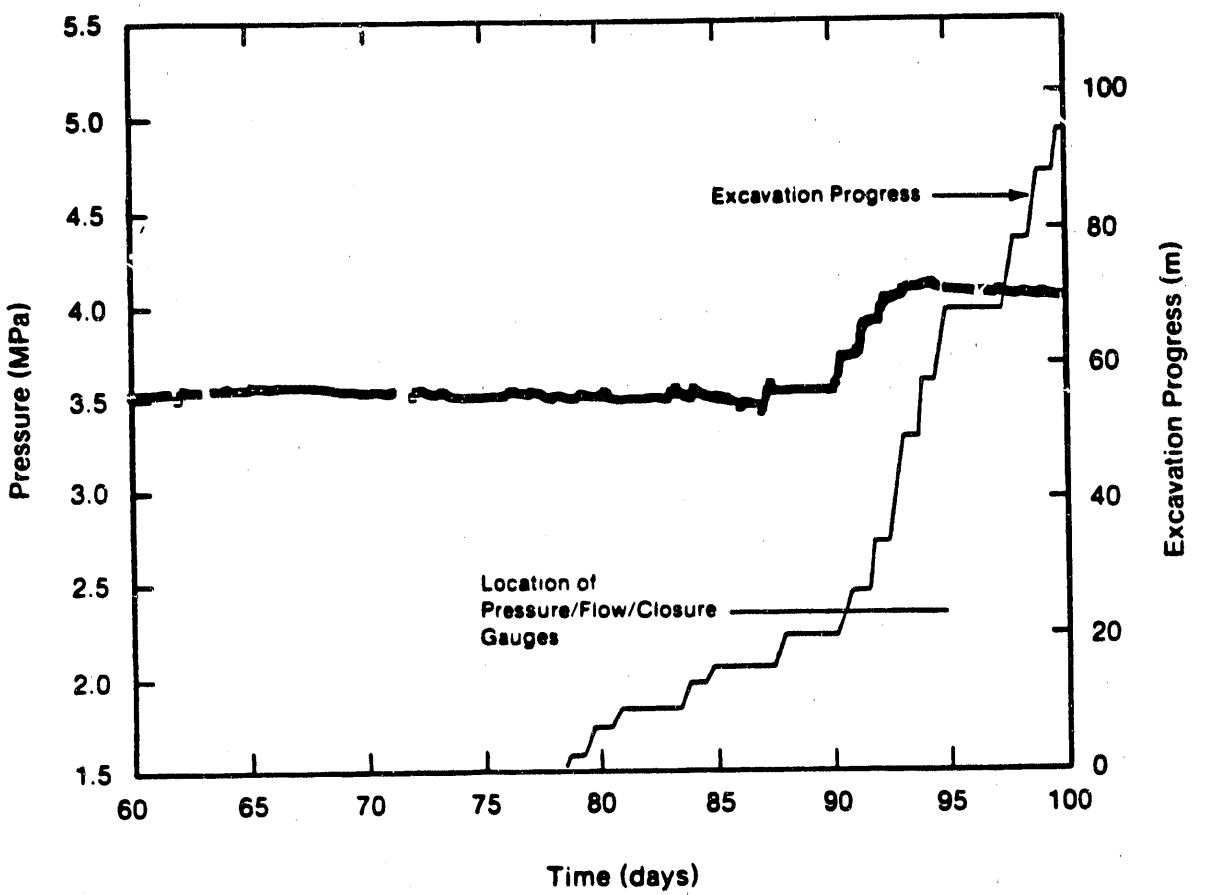

Figure 13. Test region pressure measured in borehole QPP21 during excavation of Room Q.

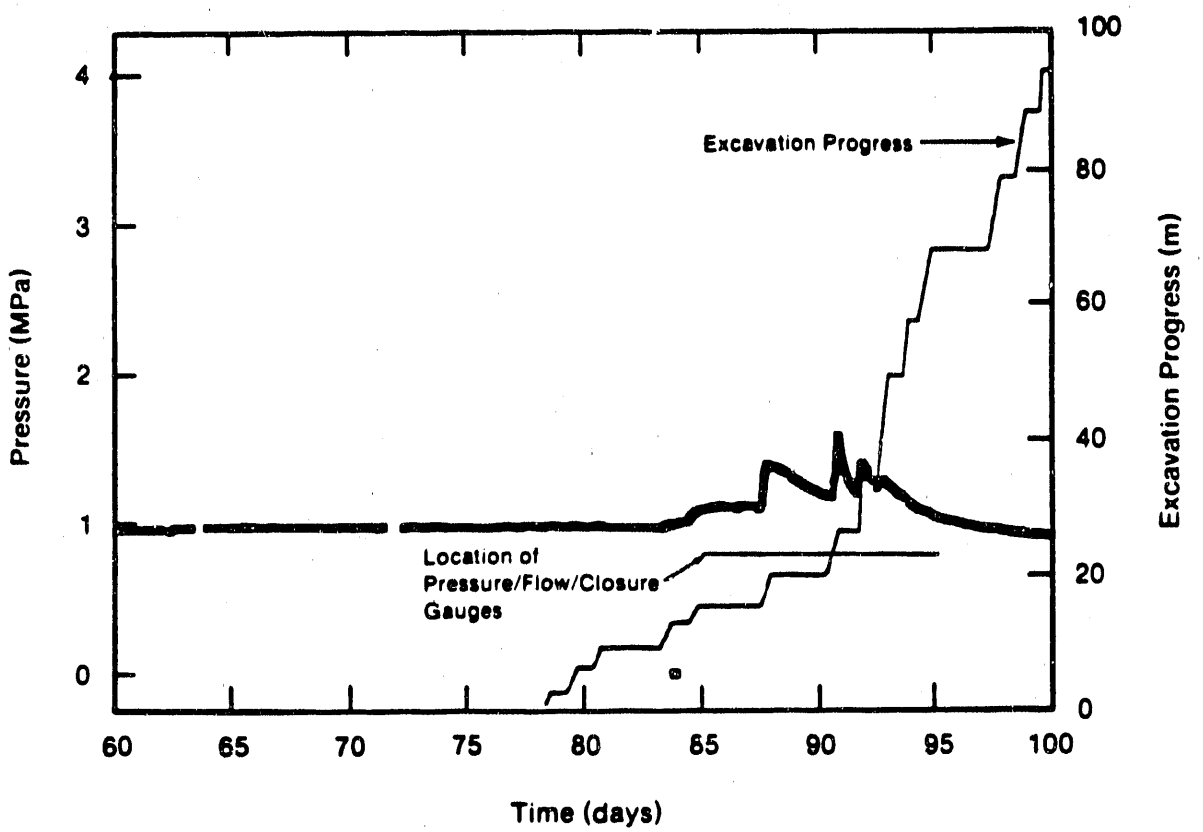

Figure 14. Test region pressure measured in borehole QPP02 during excavation of Room Q.

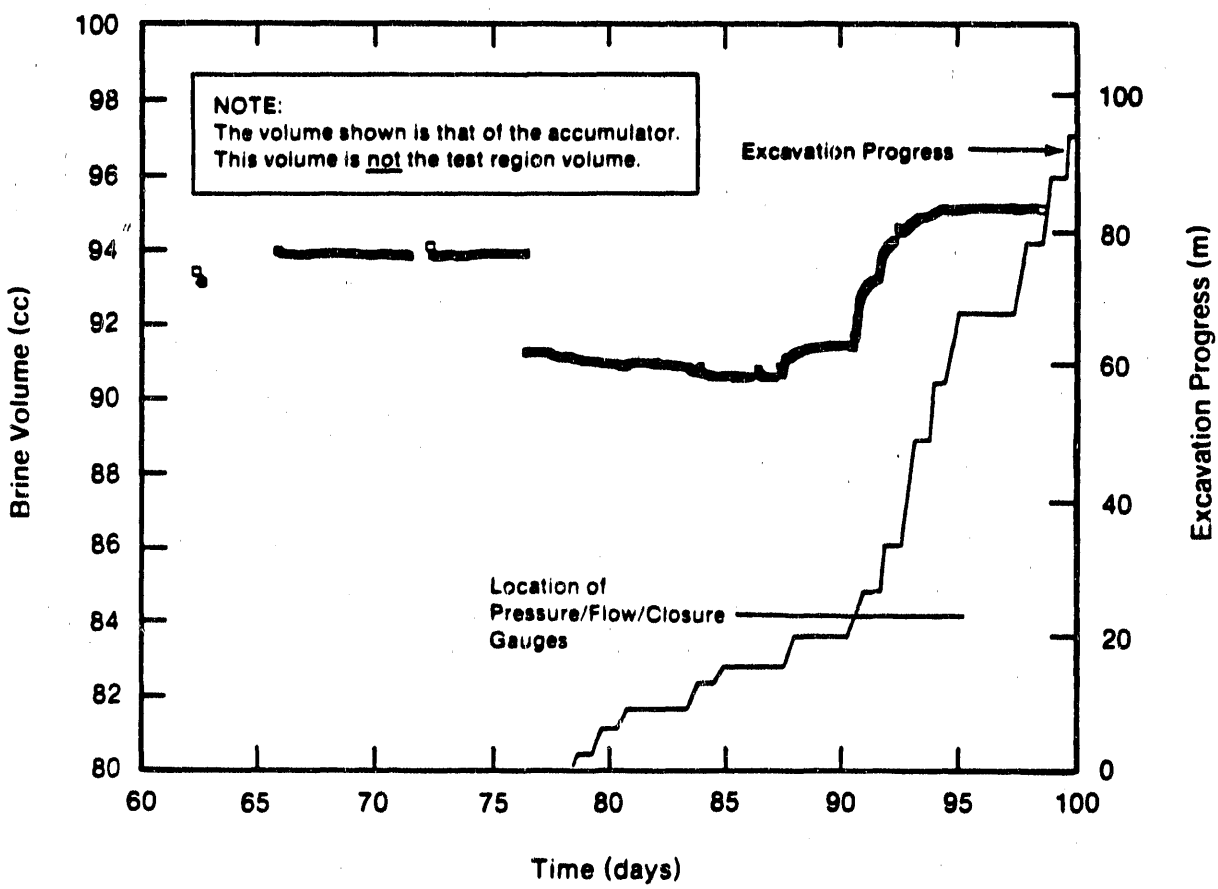

Figure 15. Test region brine volume measured in borehole QPP23 during excavation of Room Q.

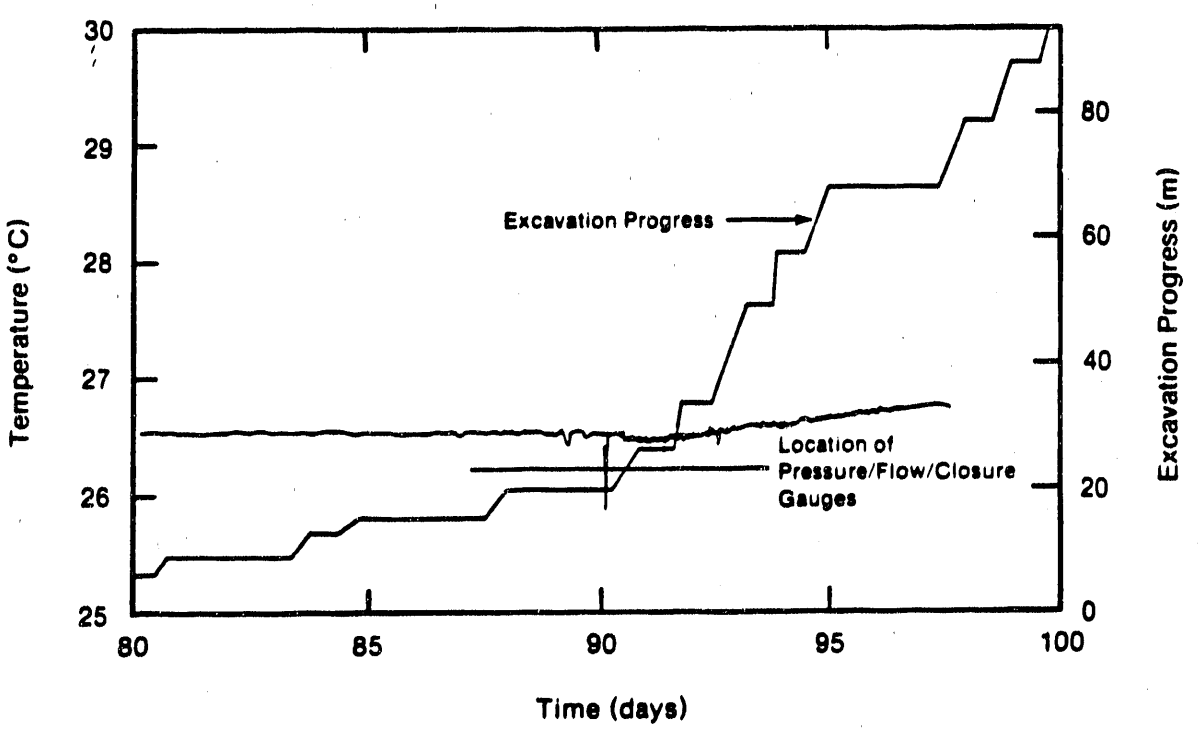

TRI-6344-500-0

Figure 16. Temperature history at borehole QPP03 test area.

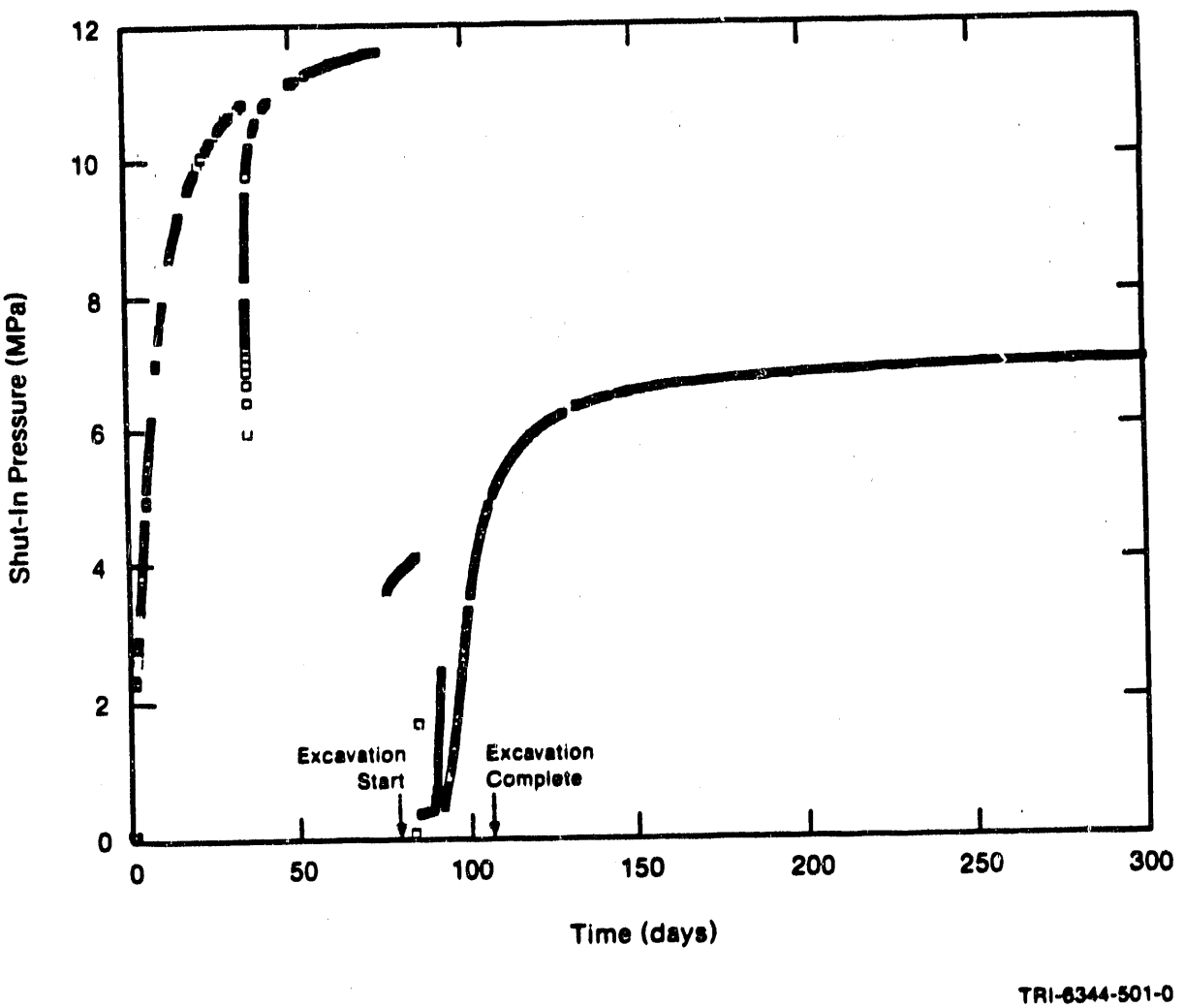

Figure 17. QPP03 pre- and post-excavation test region shut-in pressure data.

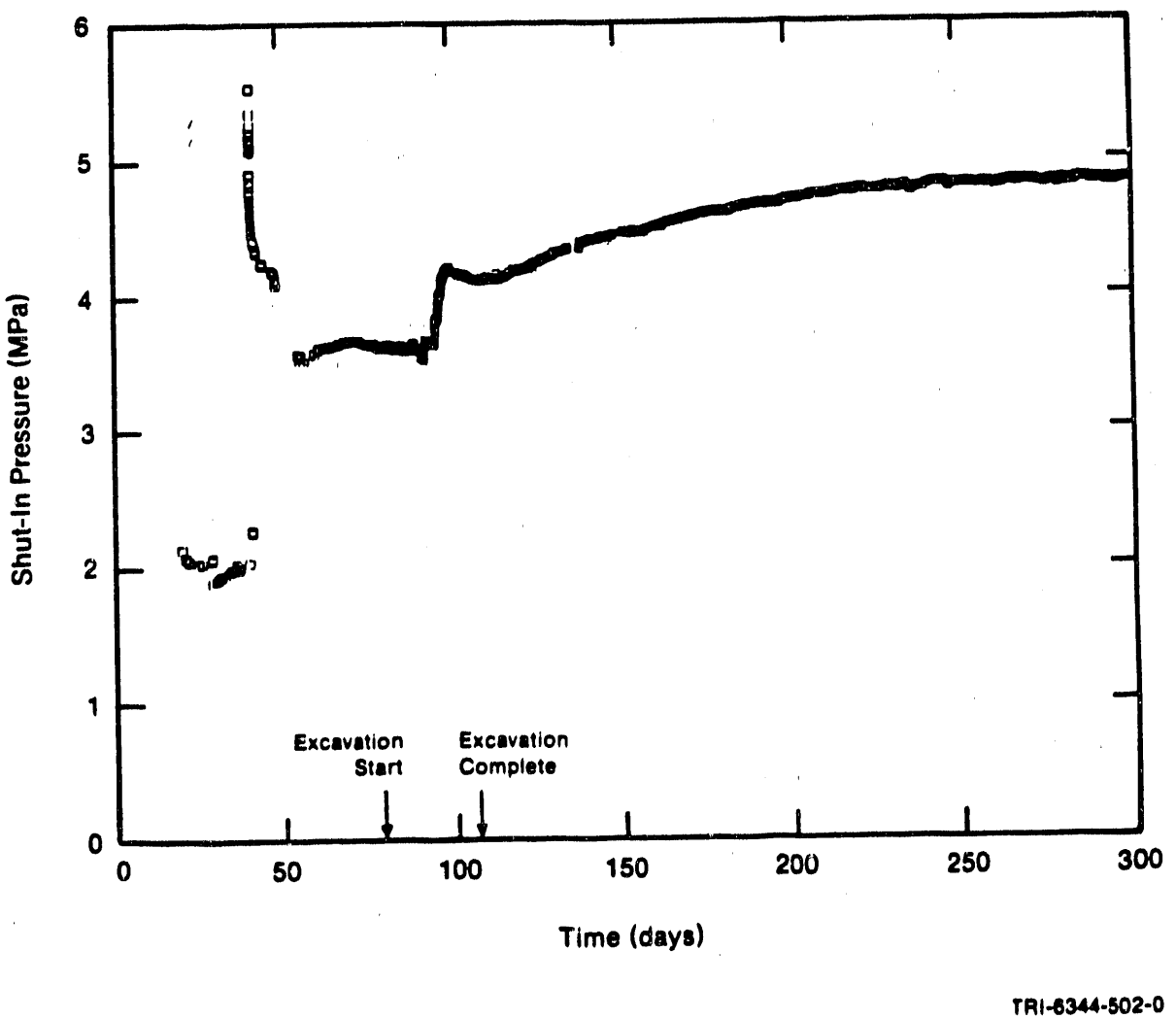

Figure 18. QPP21 pre- and post-excavation shut-in pressure data.

END

DATE FILMED

03/06/91